CATT TECHNICAL REPORT No. 02-02-01

Adaptive Sliding Mode Control Design for A Hypersonic Flight Vehicle

Haojian Xu[*], Petros A. Ioannou[†]
University of Southern California, Los Angeles, CA 90089
and
Majdedin Mirmirani[‡]
California State University, Los Angeles, CA 90032

A Multi Input Multi Output (MIMO) adaptive sliding controller is designed and analyzed for the longitudinal dynamics of a generic hypersonic air vehicle. This vehicle model is highly nonlinear, multivariable, unstable and includes 6 uncertainty parameters. Simulation studies were conducted for trimmed cruise conditions of 110,000 ft and Mach 15 where the responses of the vehicle to a step change in altitude and airspeed were evaluated. The commands were 100ft/s step-velocity and 2000ft step-altitude. The controller is evaluated for robustness will respect to parameter uncertainties using simulations. These simulation studies demonstrate that the proposed controller meets the performance requirements with relatively low amplitude control inputs despite parameter uncertainties.

Nomenclature

a	Speed of Sound, ft/s
C_D	Drag Coefficient
C_L	Lift Coefficient
$C_M(q)$	Moment Coefficient due to Pitch Rate
$C_M(\alpha)$	Moment Coefficient due to Angle of Attack
$C_M(\delta_e)$	Moment Coefficient due to Elevator Deflection
C_T	Thrust Coefficient
$\bar{c}$	Reference Length, ft
D	Drag, lbf
h	Altitude, ft
I_{yy}	Moment of Inertia, slug-ft^2
L	Lift, lbf
M	Mach Number
M_{yy}	Pitching Moment, lbf-ft
m	Mass, slugs
q	Pitch Rate, rad/s
R_E	Radius of the Earth, ft

[*] Graduate student, Department of Electrical Engineering-Systems.
[†] Professor, Department of Electrical Engineering-Systems.
[‡] Professor, Department of Mechanical Engineering. Member AIAA.

r	Radial Distance from Earth's center, ft
S	Reference Area, ft^2
T	Thrust, lbf
V	Velocity, ft/s
α	Angle of Attack, rad
β	Throttle Setting
γ	Flight-Path Angle, rad
δ_e	Elevator Deflection, rad
μ	Gravitational Constant
ρ	Density of Air, $slugs/ft^3$

INTRODUCTION

Hypersonic air vehicles have a highly nonlinear dynamics and because of their design and flight conditions of high altitudes and Mach numbers, they are extremely sensitive to changes in atmospheric conditions as well as physical and aerodynamic parameters. As the result, modeling inaccuracies can have strong adverse effects on the performance of air vehicle's control systems. Therefore, robust control has been the main technique used for hypersonic flight control (Refs. 1-2).

The sliding mode control method provides a systematic approach to the problem of maintaining stability and consistent performance in the face of modeling imprecision. The main advantage of the sliding mode control is that system's response remains insensitive to model uncertainties and disturbances (Refs. 3-4). The most completely developed area of sliding mode control is for single-input single-output systems (SISO) (Ref. 3). In Ref. 4 SISO sliding mode control is extended to a class of nonlinear MIMO systems. Although the technique has excellent robustness properties, pure sliding mode control presents several drawbacks including large control authority and chattering. The performance of the pure sliding mode control can be improved by coupling it with an on-line parameter estimation scheme (Ref. 5). Also, a sliding mode controller can be implemented only if full state feedback is available, a requirement not readily achieved in a hypersonic flight. The design of a state observer for the unmeasurable states based on sliding modes has been proposed in Ref. 6, where it is shown that sliding mode observers have an inherent robustness in the face of parametric uncertainty and measurement noise. An adaptive sliding controller combined with an observer was applied to a SISO magnetic suspension system in Ref. 7 and to a linear MIMO robotic system in Ref. 8.

In this paper the design a MIMO adaptive controller for a hypersonic air vehicle based on the sliding mode control technique is presented. The plant is the longitudinal model of a generic hypersonic air vehicle (Refs. 1-2). This model is nonlinear, multivariable, and unstable and includes uncertainty in aerodynamic parameters. The open-loop dynamics of the air vehicle exhibits unstable short-period and height modes, as well as a lightly damped phugoid mode. The control design described in the following sections consists of 4 steps. First, a full-state feedback is applied to linearize the dynamics of the air vehicle with respect to air speed, V, and altitude, h. Next, a pure sliding controller is designed. An adaptive sliding controller is then designed to improve performance in the presence of parametric uncertainty. In addition, a sliding observer is designed to estimate the angle of attack and the flight path angel, which are difficult to measure in a hypersonic flight. Finally, the complete controller is synthesized by combining the adaptive controller and the observer. Simulation studies were conducted for trimmed cruise conditions of 110,000 ft and Mach 15 to evaluate the response of the vehicle to a step change of 2000 ft in altitude and 100 ft/sec in airspeed. Parameter uncertainties were included in the aerodynamics coefficients and were allowed to take their maximum possible deviation in the simulation studies. The results showed that the combined adaptive sliding controller is robust and provides good performance with limited control authority under the conditions of parametric uncertainty over the entire flight envelope.

HYPERSONIC AIR VEHICLE MODEL

A model for the longitudinal dynamics of a generic hypersonic vehicle was presented in Refs. 1and 2. The equations of motion developed include an inverse-square-law gravitational model, and the centripetal acceleration. In this study we have used a modified version of the same model by making appropriate simplifications in the aerodynamical coefficients. The nominal flight of the vehicle is at trimmed cruise condition (M=15, V=15,060 ft/s, h=110,000 ft, γ=0 deg, and q=0 deg/s). The equations of motion describing the model are:

$$\dot{V} = \frac{T\cos\alpha - D}{m} - \frac{\mu \sin\gamma}{r^2} \tag{1}$$

$$\dot{\gamma} = \frac{L + T\sin\alpha}{mV} - \frac{(\mu - V^2 r)\cos\gamma}{Vr^2} \tag{2}$$

$$\dot{h} = V\sin\gamma \tag{3}$$

$$\dot{\alpha} = q - \dot{\gamma} \tag{4}$$

$$\dot{q} = M_{yy} / I_{yy} \tag{5}$$

where

$$L = \tfrac{1}{2}\rho V^2 S C_L \tag{6}$$

$$D = \tfrac{1}{2}\rho V^2 S C_D \tag{7}$$

$$T = \tfrac{1}{2}\rho V^2 S C_T \tag{8}$$

$$M_{yy} = \tfrac{1}{2}\rho V^2 S\bar{c}[C_M(\alpha) + C_M(\delta_e) + C_M(q)] \tag{9}$$

$$r = h + R_E \tag{10}$$

$$C_L = 0.6203\alpha \tag{11}$$

$$C_D = 0.6450\alpha^2 + 0.0043378\alpha + 0.003772 \tag{12}$$

$$C_T = \begin{cases} 0.02576\beta & \text{if } \beta < 1 \\ 0.0224 + 0.00336\beta & \text{if } \beta > 1 \end{cases} \tag{13}$$

$$C_M(\alpha) = -0.035\alpha^2 + 0.036617\alpha + 5.3261\times 10^{-6} \tag{14}$$

$$C_M(q) = (\bar{c}/2V)q(-6.796\alpha^2 + 0.3015\alpha - 0.2289) \tag{15}$$

$$C_M(\delta_e) = c_e(\delta_e - \alpha) \tag{16}$$

The engine dynamics are modeled by a second order system:

$$\ddot{\beta} = -2\zeta\omega_n\dot{\beta} - \omega_n^2\beta + \omega_n^2\beta_c \tag{17}$$

Parameter uncertainties are modeled as an additive variance, Δ, to the nominal values which used for control design, i.e.,

$$m = 9375(1 + \Delta m) \tag{18}$$

$$I_{yy} = 7(1 + \Delta I)\times 10^6 \tag{19}$$

$$S = 3603(1 + \Delta S) \tag{20}$$

$$\bar{c} = 80(1 + \Delta\bar{c}) \tag{21}$$

$$c_e = 0.0292(1+\Delta c_e) \tag{22}$$

$$\rho = 0.24325(1+\Delta c_\rho)\times 10^{-4} \tag{23}$$

The maximum values of additive uncertainties used in the simulation studies are taken as follows:

$$|\Delta m| \le 0.03\ ;\ |\Delta I| \le 0.02\ ;\ |\Delta S| \le 0.03\ ;\ |\Delta \bar{c}| \le 0.02\ ;\ |\Delta c_e| \le 0.02\ ;\ |\Delta c_\rho| \le 0.03 \tag{24}$$

The control inputs are the throttle setting, β_c, and the elevator deflection, δ_e. The outputs are the velocity, V, and the altitude, h. The commanded desired values of velocity and altitude are denoted by, V_d and h_d respectively.

INPUT-OUTPUT LINEARIZATION

The longitudinal model of the generic hypersonic air vehicle described by Eqs. (1-5) is a special case of a general MIMO nonlinear system of the form

$$\dot{\boldsymbol{x}}(t) = \boldsymbol{f}(\boldsymbol{x}) + \sum_{k=1}^{m} \boldsymbol{g}_k(\boldsymbol{x}) u_k \tag{25}$$

$$y_i(t) = h_i(\boldsymbol{x}),\quad i=1,\ldots,m \tag{26}$$

where $\boldsymbol{f}$, $\boldsymbol{g}$, $\boldsymbol{h}$ are sufficiently smooth functions in $\Re^n$. Input-Output linearization uses full state feedback to globally linearize the nonlinear dynamics of selected controlled outputs. Following the approach in Ref. 4, each of the output channels y_i is differentiated a sufficient number of times until a control input component appears in the resulting equation. Let r_i, the linearizability index, be the minimum order of the derivative of y_i for which the coefficient of at least one u_k is not zero. Using the Lie derivative notation this derivative can be expressed as:

$$y_i^{(r_i)} = L_{\boldsymbol{f}}^{r_i}(h_i) + \sum_{k=1}^{m} L_{\boldsymbol{g}_k}(L_{\boldsymbol{f}}^{r_i-1}(h_i))u_k \tag{27}$$

where the Lie derivatives are defined as:

$$L_{\boldsymbol{f}}(h_i) = \frac{\partial h_i}{\partial x_1} f_1 + \cdots + \frac{\partial h_i}{\partial x_n} f_n$$

$$L_{\boldsymbol{f}}^{r}(h_i) = L_{\boldsymbol{f}}(L_{\boldsymbol{f}}^{r-1}(h_i))$$

$$L_{\boldsymbol{g}_k}(h_i) = \frac{\partial h_i(\boldsymbol{x})}{\partial \boldsymbol{x}} \boldsymbol{g}_k$$

Given that the nonlinear system is I/O linearizable, for each output y_i there exists a linearizability index r_i. Accordingly, $r = \sum_{i=1}^{m} r_i$ is called the relative degree of the nonlinear system. The necessary and sufficient condition for the existence of a transformation linearizing the system completely from the I/O point of view is that the relative degree, r, be the same as the order of the system, n, i.e., r=n. If $r < n$, however, the nonlinear system can only be partially linearized. In this case, the stability of the nonlinear system given by Eqs. (25-26) also depends on the stability of the internal dynamics (zero dynamics).

Applying the above technique to the longitudinal model of the hypersonic vehicle, the output dynamics for velocity V and altitude h can be derived by differentiating V three times and h four times as seen below. Therefore the relative degree of the system, r=3+4=7=n, equals to the order of the system. Hence, the nonlinear longitudinal model can be linearized completely and the closed-loop system will have no zero dynamics (Ref. 2). The linearized model can be developed by repeated differentiation of V and h as follows:

$$\dot{V} = f_1(\boldsymbol{x})$$
$$\ddot{V} = \omega_1 \dot{\boldsymbol{x}} / m$$
$$\dddot{V} = (\omega_1 \ddot{\boldsymbol{x}} + \dot{\boldsymbol{x}} \Omega_2 \dot{\boldsymbol{x}}) / m \tag{28}$$

$$\ddot{h} = \dot{V} \sin\gamma + V\dot{\gamma}\cos\gamma$$
$$\dddot{h} = \ddot{V} \sin\gamma + 2\dot{V}\dot{\gamma}\cos\gamma - V\dot{\gamma}^2 \sin\gamma + V\ddot{\gamma}\cos\gamma$$
$$h^{(4)} = \dddot{V} \sin\gamma + 3\ddot{V}\dot{\gamma}\cos\gamma - 3\dot{V}\dot{\gamma}^2 \sin\gamma + 3\dot{V}\ddot{\gamma}\cos\gamma - 3V\dot{\gamma}\ddot{\gamma}\sin\gamma - V\dot{\gamma}^3 \cos\gamma + V\dddot{\gamma}\cos\gamma \tag{29}$$

In Eq. (29)

$$\dot{\gamma} = f_2(\boldsymbol{x})$$
$$\ddot{\gamma} = \pi_1 \dot{\boldsymbol{x}}$$
$$\dddot{\gamma} = \pi_1 \ddot{\boldsymbol{x}} + \dot{\boldsymbol{x}}^T \Pi_2 \dot{\boldsymbol{x}} \tag{30}$$

where $\boldsymbol{x}^T = \begin{bmatrix} V & \gamma & \alpha & \beta & h \end{bmatrix}$, f_1 and f_2 are the short hand expressions of the right-hand-side of Eqs. (1) and (2) respectively, and $\omega_1 = \partial f_1(\boldsymbol{x}) / \partial \boldsymbol{x}$, $\Omega_2 = \partial \omega_1 / \partial \boldsymbol{x}$. The detailed expressions for ω_1, Ω_2, π_1, and Π_2 can be found in (Ref. 2). The expression of the second derivatives for α and β can be viewed as consisting of two parts: a part that is control relevant and a part that is not.

$$\ddot{\alpha} = \ddot{\alpha}_0 + (c_e \rho V^2 S\bar{c} / 2I_{yy})\delta_e \tag{31}$$
$$\ddot{\beta} = \ddot{\beta}_0 + \omega_n^2 \beta_{com} \tag{32}$$

where

$$\ddot{\alpha}_0 = \tfrac{1}{2}\rho V^2 S\bar{c}[C_M(\alpha) + C_M(q) - c_e\alpha] / I_{yy} - \ddot{\gamma} \tag{33}$$
$$\ddot{\beta}_0 = -2\zeta\omega_n \dot{\beta} - \omega_n^2 \beta \tag{34}$$

Defining $\ddot{\boldsymbol{x}}_0^T = [\dddot{V} \quad \ddot{\gamma} \quad \ddot{\alpha}_0 \quad \ddot{\beta}_0 \quad \ddot{h}]$, the output dynamics of V and h can be written as:

$$\dddot{V} = \dddot{V}_0 + b_{11}\beta_c + b_{12}\delta_e \tag{35}$$
$$h^{(4)} = h_0^{(4)} + b_{21}\beta_c + b_{22}\delta_e \tag{36}$$

which, includes control inputs, β_c, δ_e, explicitly and where,

$$\dddot{V}_0 = (\omega_1 \ddot{\boldsymbol{x}}_0 + \dot{\boldsymbol{x}}\Omega_2 \dot{\boldsymbol{x}}) / m \tag{37}$$
$$\begin{aligned} h_0^{(4)} &= 3\ddot{V}\dot{\gamma}\cos\gamma - 3\dot{V}\dot{\gamma}^2 \sin\gamma + 3\dot{V}\ddot{\gamma}\cos\gamma - 3V\dot{\gamma}\ddot{\gamma}\sin\gamma - V\dot{\gamma}^3\cos\gamma \\ &\quad + (\omega_1 \ddot{\boldsymbol{x}}_0 + \dot{\boldsymbol{x}}^T \Omega_2 \dot{\boldsymbol{x}})\sin\gamma / m + V\cos\gamma(\pi_1 \ddot{\boldsymbol{x}}_0 + \dot{\boldsymbol{x}}^T \Pi_2 \dot{\boldsymbol{x}}) \end{aligned} \tag{38}$$
$$b_{11} = (\rho V^2 S c_\beta \omega_n^2 / 2m)\cos\alpha \tag{39}$$
$$b_{12} = -(c_e \rho V^2 S\bar{c} / 2mI_{yy})(T\sin\alpha + D_\alpha) \tag{40}$$
$$b_{21} = (\rho V^2 S c_\beta \omega_n^2 / 2m)\sin(\alpha + \gamma) \tag{41}$$
$$b_{11} = (c_e \rho V^2 S\bar{c} / 2mI_{yy})[T\cos(\alpha+\gamma) + L_\alpha \cos\gamma - D_\alpha \sin\gamma] \tag{42}$$
$$D_\alpha = \partial D / \partial\alpha \text{, and } L_\alpha = \partial L / \partial\alpha \tag{43}$$
$$c_\beta = \partial C_T / \partial\beta = \begin{cases} 0.02576, & \beta < 1 \\ 0.00336, & \beta > 1 \end{cases} \tag{44}$$

THE SLIDING MODE CONTROLLER DESIGN

The control design problem is to select a vector $[\beta_c \quad \delta_e]^T$ that forces the velocity V and altitude h to track the desired commanded values V_d and h_d in the presence of parametric uncertainty. By applying the techniques introduced in Ref. 4, first two decoupled sliding surfaces s_1 and s_2 are chosen:

$$s_1 = (d/dt + \lambda_1)^3 \int_0^t e_1(\tau) d\tau \; ; \qquad e_1(t) = V - V_d \tag{45}$$

$$s_2 = (d/dt + \lambda_2)^4 \int_0^t e_2(\tau) d\tau \; ; \qquad e_2(t) = h - h_d \tag{46}$$

where λ_1 and λ_2 are strictly positive constants defining the bandwidth of the error dynamics. The sliding surfaces $s_i = 0$, i=1,2 represent linear differential equations whose solutions imply $\int e_i(t)$, i=1,2 approach zero exponentially with the time constants $2/\lambda_1$ and $3/\lambda_2$ respectively (Ref. 3), where the integrals of the tracking errors are used to cancel the steady state errors (Ref. 3).

Differentiating s_1 and s_2, we have:

$$\dot{s}_1 = -\dddot{V}_d + \dddot{V}_0 + 3\lambda_1 \ddot{e}_1 + 3\lambda_1^2 \dot{e}_1 + \lambda_1^3 e_1 + b_{11}\beta_c + b_{12}\delta_e \tag{47}$$

$$\dot{s}_2 = -h_d^{(4)} + h_0^{(4)} + 4\lambda_2 e_2^{(3)} + 6\lambda_2^2 \ddot{e}_2 + 4\lambda_2^3 \dot{e}_2 + \lambda_2^4 e_2 + b_{21}\beta_c + b_{22}\delta_e \tag{48}$$

Eqs. (47) and (48) can be written in compact vector format as:

$$\begin{bmatrix} \dot{s}_1 \\ \dot{s}_2 \end{bmatrix} = \begin{bmatrix} v_1(\boldsymbol{x}) \\ v_2(\boldsymbol{x}) \end{bmatrix} + \begin{bmatrix} b_{11} & b_{12} \\ b_{21} & b_{22} \end{bmatrix} \begin{bmatrix} \beta_c \\ \delta_e \end{bmatrix} \tag{49}$$

where,

$$v_1(\boldsymbol{x}) = -\dddot{V}_d + 3\lambda_1 \ddot{e}_1 + 3\lambda_1^2 \dot{e}_1 + \lambda_1^3 e_1 \tag{50}$$

$$v_2(\boldsymbol{x}) = -h_d^{(4)} + 4\lambda_2 e_2^{(3)} + 6\lambda_2^2 \ddot{e}_2 + 4\lambda_2^3 \dot{e}_2 + \lambda_2^4 e_2 \tag{51}$$

The sliding control design is choosing control inputs such that the following attractive equations are satisfied.

$$\dot{s}_1 = -k_1 \operatorname{sgn}(s_1) \tag{52}$$

$$\dot{s}_2 = -k_2 \operatorname{sgn}(s_2) \tag{53}$$

where k_1 and k_2 are strictly positive constants whose choice determines the desired reaching time to the sliding surfaces. The above attractive equations, also called sliding conditions, imply that the "distance" to the sliding surface decreases along all system trajectories. Furthermore, the sliding condition makes the sliding surfaces an invariant set, i.e., once systems trajectories reaches the surface, it will remain on it for the rest of the time. In addition, for any initial condition, the sliding surface will be reached in a finite time (Ref. 3).

Using (49) the controller that satisfies the sliding conditions (52) and (53) is given by:

$$\begin{bmatrix} \beta_c \\ \delta_e \end{bmatrix} = B^{-1} \begin{bmatrix} -v_1(\mathrm{x}) - k_1 \operatorname{sgn}(s_1) \\ -v_2(\mathrm{x}) - k_2 \operatorname{sgn}(s_2) \end{bmatrix}, \quad B = \begin{bmatrix} b_{11} & b_{12} \\ b_{21} & b_{22} \end{bmatrix} \tag{54}$$

Here, B is assumed to be invertible. It is easy to see that B inverse indeed exists for the entire flight envelop except a vertical flight path (Ref. 2). Therefore, the sliding controller is valid over the entire flight envelope. The control law in Eq. (54) can be viewed as consisting of two parts: the term $-B^{-1}[v_1 \quad v_2]^T$, is called the equality control, which guarantees $\dot{s}_i = 0$, i=1,2 for the nominal model, and the other term, $-B^{-1}[k_1 \operatorname{sgn}(s_1) \quad k_2 \operatorname{sgn}(s_2)]$, is incorporated to deals with parameter uncertainties. With this design, the sliding surfaces will be reached even in the presence of parameter uncertainties. In fact, when the parameter uncertainty exists, the actual attractiveness equations are given by:

$$\begin{bmatrix} \dot{s}_1 \\ \dot{s}_2 \end{bmatrix} = \begin{bmatrix} \Delta\dddot{V}_0 + v_1 \\ \Delta h_0^{(4)} + v_2 \end{bmatrix} + (\Delta B) B\boldsymbol{u} = \begin{bmatrix} -k_1 \operatorname{sgn}(s_1) \\ -k_2 \operatorname{sgn}(s_2) \end{bmatrix}$$

in which k_i's can be chosen large enough to guarantee that $\dot{s}_i < 0$, i=1,2. However, in the presence of large uncertainties, k_i's may have to be chosen so large, which imply a large control effort. Also, due to the discontinuity across the sliding surfaces, the above control law may introduce the so-called chattering. The discontinuity in the control law can be made continuous by defining two thin boundary layers of widths Φ_1 and Φ_2 around the sliding surfaces, i.e., substituting $\text{sgn}(s_i)$ with saturation functions $\text{sat}(s_i / \Phi_i)$, i=1,2. where,

$$\text{sat}(x) = \begin{cases} x, & x \le 1 \\ \text{sgn}(x), & \text{otherwise} \end{cases}$$

With this scheme the control law achieves a trade-off between tracking precision and robustness required for control in the presence of uncertainty. Analysis demonstrated by simulations shows that both the sliding surfaces and the attractive conditions influence how fast the system responds to a step input (Ref. 4).

Also, in order to guarantee closed loop stability, it is necessary to identify the condition where the maximum effect of the combined parameter uncertainties is encountered. Both analytical and simulation studies conducted revealed that the closed loop system is far more sensitive to variation in the gain matrix, ΔB than it is to $\Delta \boldsymbol{\nu}$. To calculate ΔB under the worst case, the gain matrix is written as a product of a fixed basis matrix Y and an uncertainty parameter matrix.

$$B = \begin{bmatrix} (1/a)Y_{11} & (1/b)Y_{12} \\ (1/a)Y_{21} & (1/b)Y_{22} \end{bmatrix} = \begin{bmatrix} Y_{11} & Y_{12} \\ Y_{21} & Y_{22} \end{bmatrix} \begin{bmatrix} (1/a) & 0 \\ 0 & (1/b) \end{bmatrix} \tag{55}$$

where,

$$a = 2\times 10^{-4} m / \rho S c_\beta \omega_n^2 \tag{56}$$

$$b = 4\times 10^{-14} (I_{yy} m) / \rho^2 S^2 c_e \bar{c} \tag{57}$$

$$Y_{11} = V^2 \cos\alpha \times 10^{-4} \tag{58}$$

$$Y_{21} = V^2 \sin(\alpha+\gamma) \times 10^{-4} \tag{59}$$

$$Y_{12} = -V^4 (C_T \sin\alpha + \partial C_D / \partial\alpha) \times 10^{-14} \tag{60}$$

$$Y_{22} = V^4 \{C_T \cos(\alpha+\gamma) + (\partial C_L / \partial\alpha)\cos\gamma - (\partial C_D / \partial\alpha)\sin\gamma\} \times 10^{-14} \tag{61}$$

Constants, a and b, embody the combinations of all uncertainty parameters in B. The worse case occurs when Δm and ΔI take their maximum negative values, while Δc_ρ, ΔS, Δc_e, and $\Delta \bar{c}$ take their maximum positive values. The uncertainties in $\ddot{V}_0$ and $h_0^{(4)}$ are a nonlinear combinations of the uncertainty parameters. Using a Taylor series expansion of these terms around their nominal values and neglecting the high order error terms, the terms $\Delta\ddot{V}_0$ and $\Delta h_0^{(4)}$ can be estimated from their nominal values.

The simulation results are shown in Figures 1-4. Figures 1 and 2 show the response of the nominal model, i.e., no uncertainties. In Figure 1, the vehicle responses to a 100 ft/s step velocity command at the trimmed condition. It is observed that the velocity converges to the desired value in a short time while the altitude remains almost unchanged. Figure 2 depicts the vehicle response to a 2000 ft step altitude command. Similarly, the altitude converges to its desired value with a short response time. In both cases the controller achieves quick convergence, no overshoot, and no steady state error for the nominal model. Figures 3 and 4 show the simulation results for the same maneuvers in the presence of maximum parameter uncertainty. The results show that robustness and stability have indeed been achieved. The price paid to achieve robustness in this case is in the form of large gains k_1 and k_2. Furthermore, the exact tracking can only be realized by extremely high control switching activity. The widths of the boundary layers have to be expanded resulting in steady sate errors. Thus, in the presence of uncertainties, exact tracking is not achievable by the application of a pure sliding mode controller. This drawback of the sliding mode controller is removed in the next section where an on-line parameter estimator is combined with the sliding mode controller in order to take care of the parametric uncertainty.

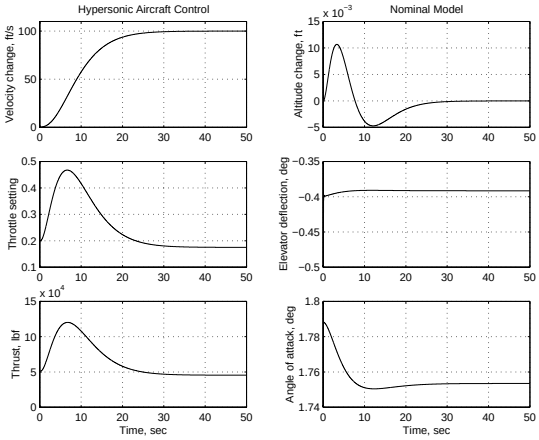

Figure 1 Response To A 100ft/s Step Velocity Command For Nominal Model

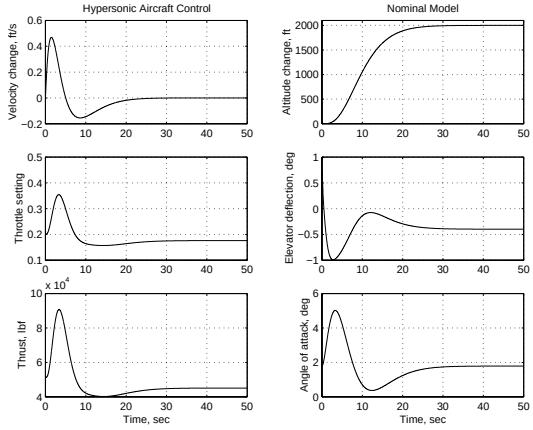

Figure 2 Response To A 2000ft Step Altitude Command For Nominal Model

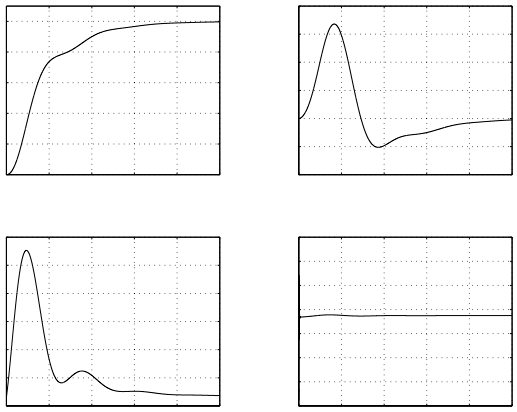

Figure 3 Response To A 100ft/s Step Velocity Command With Maximum Parameter Uncertainties

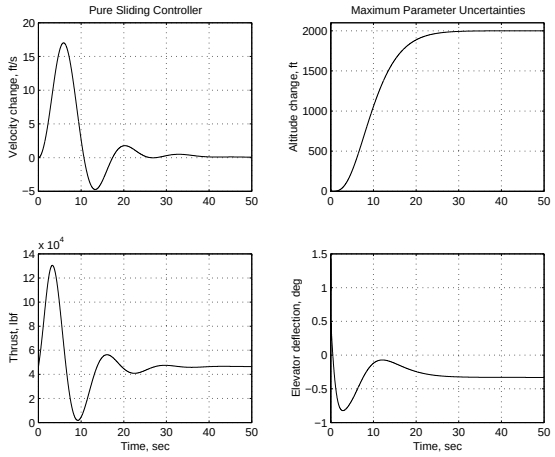

Figure 4 Response To A 2000ft Step Altitude Command With Parameter Uncertainties

ADAPTIVE SLIDING MODE CONTROLLER DESIGN

As demonstrated in the previous section, the sliding mode controller achieves good tracking in the presence of parametric uncertainty at the expense of high gain control inputs. The performance of the sliding mode controller is dependent on the size of the parametric uncertainties involved. An undesirable characteristic of this controller is to have to balance performance with robustness. This shortcoming of the pure sliding controller has motivated combining the above control law with on line parameter adaptation. In this section we develop an adaptive sliding mode controller, which combines an on-line parameter estimator with the sliding mode controller of the previous section. The adaptive laws for updating parameters are generated using the Lyapunov synthesis approach (Ref. 9). As mentioned before, the dynamics of the system is more sensitive to the uncertainty parameters in the gain matrix *B*. The gain matrix *B* itself is the product of a fixed basis matrix *Y* and a diagonal matrix with two parameters *a* and *b* involving uncertainties. The constant, *a*, embodies the combination of a number of uncertain parameters including *S*, c_β, ρ, $\bar{c}$, I_{yy} and *m*. and the constant, *b*, embodies the combination of uncertain parameters $\bar{c}$, *S*, c_e, ρ, I_{yy} and *m*. For a hypersonic vehicle, these parameters are fixed and strictly positive but difficult to measure exactly at any given time. In order to take care of the parametric uncertainty we combine the sliding mode controller with an on-line parameter estimator forming an adaptive sliding mode controller as described below:

$$\begin{bmatrix} \beta_c \\ \delta_e \end{bmatrix} = \begin{bmatrix} \hat{a} & 0 \\ 0 & \hat{b} \end{bmatrix} \begin{bmatrix} Y_{11} & Y_{12} \\ Y_{21} & Y_{22} \end{bmatrix}^{-1} \bar{\boldsymbol{u}} \tag{62}$$

$$\bar{\boldsymbol{u}} = \begin{bmatrix} -v_1 - k_1 \,\mathrm{sat}(s_1 / \Phi_1) \\ -v_2 - k_2 \,\mathrm{sat}(s_2 / \Phi_2) \end{bmatrix} \tag{63}$$

where $\hat{a}$ and $\hat{b}$ are the on-line estimates of the uncertain parameters *a* and *b*.

The adaptive laws can be derived using the Lyapunov synthesis approach. Consider the Lyapunov-like function:

$$V = \frac{1}{2}\boldsymbol{s}_\Delta^T \boldsymbol{s}_\Delta + \frac{1}{2ak_a}\tilde{a}^2 + \frac{1}{2bk_b}\tilde{b}^2 \tag{64}$$

where,

$\tilde{a} = \hat{a} - a$ and $\tilde{b} = \hat{b} - b$

$\boldsymbol{s}_\Delta^T = [s_{1\Delta}\ s_{2\Delta}]$

$$s_{1\Delta} = s_1 - \Phi_1 \,\mathrm{sat}(s_1/\Phi_1)$$
$$s_{2\Delta} = s_2 - \Phi_2 \,\mathrm{sat}(s_2/\Phi_2)$$

In this construction, $\boldsymbol{s}_\Delta$ can be thought of a measure of the algebraic distances of the current states to the boundary layers. The adaptation ceases as sliding surfaces reach the boundary layers (Ref. 5). Following the treatment in Ref. 9 we have:

$$\dot{V} = \boldsymbol{s}_\Delta^T \begin{bmatrix} -\Delta\ddot{V}_0 - k_1\,\mathrm{sat}(s_1/\Phi_1) \\ -\Delta h_0^{(4)} - k_2\,\mathrm{sat}(s_2/\Phi_2) \end{bmatrix} + \boldsymbol{s}_\Delta^T \begin{bmatrix} Y_{11} & Y_{12} \\ Y_{21} & Y_{22} \end{bmatrix} \begin{bmatrix} \tilde{a}/a & 0 \\ 0 & \tilde{b}/b \end{bmatrix} \begin{bmatrix} Y_{11} & Y_{12} \\ Y_{21} & Y_{22} \end{bmatrix}^{-1} \overline{\boldsymbol{u}} + \frac{1}{ak_a}\tilde{a}\dot{\hat{a}} + \frac{1}{bk_b}\tilde{b}\dot{\hat{b}} \tag{65}$$

Eq. (65) can be further expanded as:

$$\dot{V} = -(k_1 - \left|\Delta\ddot{V}_0\right|)\left|s_{1\Delta}\right| - (k_2 - \left|\Delta h_0^{(4)}\right|)\left|s_{2\Delta}\right| + \frac{\tilde{a}}{a}\frac{1}{\Delta}\boldsymbol{s}_\Delta^T \begin{bmatrix} Y_{11}Y_{22} & -Y_{11}Y_{12} \\ Y_{21}Y_{22} & -Y_{21}Y_{12} \end{bmatrix} \overline{\boldsymbol{u}}$$
$$+ \frac{\tilde{b}}{b}\frac{1}{\Delta}\boldsymbol{s}_\Delta^T \begin{bmatrix} -Y_{12}Y_{21} & Y_{11}Y_{12} \\ -Y_{22}Y_{21} & Y_{11}Y_{22} \end{bmatrix} \overline{\boldsymbol{u}} + \frac{1}{ak_a}\tilde{a}\dot{\hat{a}} + \frac{1}{bk_b}\tilde{b}\dot{\hat{b}}$$

Then, the adaptive laws for estimating uncertain parameters can be derived as:

$$\dot{\hat{a}} = -\frac{k_a}{\Delta}\boldsymbol{s}_\Delta^T \begin{bmatrix} Y_{11}Y_{22} & -Y_{11}Y_{12} \\ Y_{21}Y_{22} & -Y_{21}Y_{12} \end{bmatrix} \overline{\boldsymbol{u}} \tag{66}$$

$$\dot{\hat{b}} = -\frac{k_b}{\Delta}\boldsymbol{s}_\Delta^T \begin{bmatrix} -Y_{12}Y_{21} & Y_{11}Y_{12} \\ -Y_{22}Y_{21} & Y_{11}Y_{22} \end{bmatrix} \overline{\boldsymbol{u}} \tag{67}$$

where $\Delta = Y_{11}Y_{22} - Y_{12}Y_{21}$ is the determinant of the matrix *Y*. The sliding gains are chosen as $k_1 \geq \left|\Delta\ddot{V}_0\right|_{\max}$, and $k_2 \geq \left|\Delta h_0^{(4)}\right|_{\max}$ such that $\dot{V} \leq 0$.

The simulation results using the adaptive sliding mode controller are shown in Figures 5-8. Comparing these with the results obtained using of the pure sliding mode controller shown in Figures 3 and 4, a significant improvement in performance is observed. It is seen that the level of the control effort in the adaptive case is significantly smaller. Figures 6 and 8 show that the parameters converge to their true values.

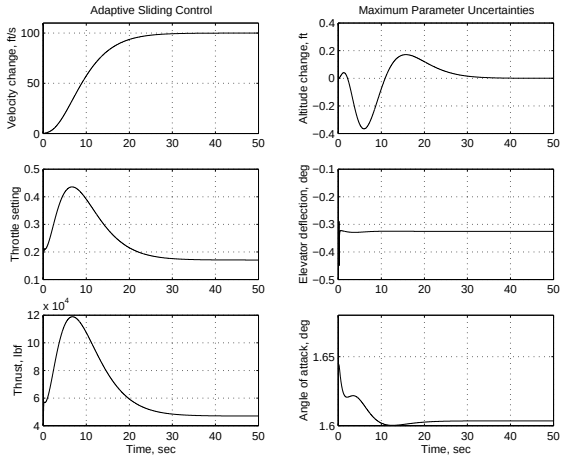

Figure 5 Adaptive Sliding Mode Controller
Response To A 100 ft/s Step Velocity Command

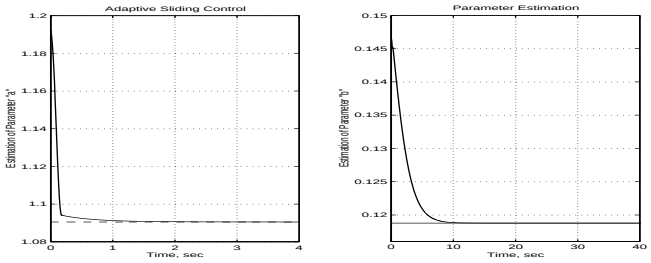

Figure 6 Parameter Estimation In Response To A 100 ft/s Step Velocity Command
True Values: a=1.0904, b=0.1188. Initial Values of Estimation: $\hat{a}(0) = 1.1926$, $\hat{b}(0) = 0.1463$

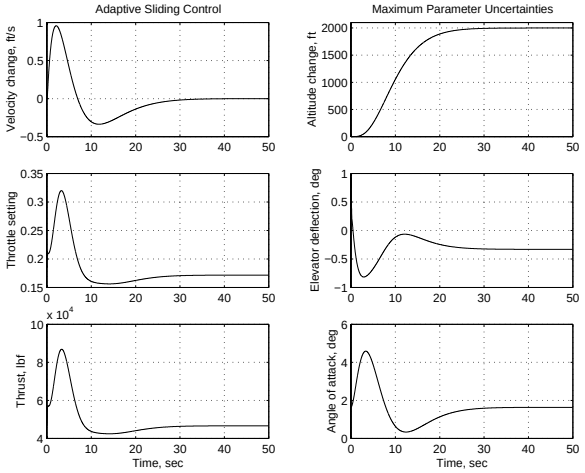

Figure 7 Adaptive Sliding Mode Controller
Response To A 2000 ft Step Command

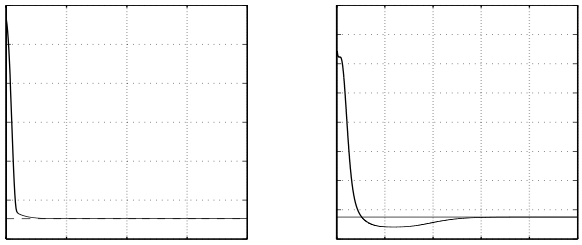

Figure 8 Parameter Estimation In Response To A 2000 ft Step Altitude Command
True Values: a=1.0904, b=0.1188. Initial Nominal Values: $\hat{a}(0) = 1.1926$, $\hat{b}(0) = 0.1463$

SLIDING MODE OBSERVER DESIGN

The sliding mode and the adaptive sliding mode controllers developed in the previous sections assume that all states are available for measurement. In reality however, only the states that correspond to velocity, V, altitude, h, and pitch rate, q, are expected to be measured. The state variables corresponding to the angle of attack, α, and flight path angle, γ, maybe difficult to measure in an actual hypersonic flight as they are generally very small. Accurate measurements are costly and difficult if at all practical possible. In this section, a sliding mode observer is designed that can provide an estimates of the angle of attack and flight

path angle based on the measurements of velocity, altitude and pitch rate. By applying the techniques developed in Ref. 6, a sliding mode observer is designed whose structure is given by Eqs. (68-71):

$$\dot{\hat{h}} = V \sin\hat{\gamma} - \alpha_1 \tilde{h} - k_h \,\mathrm{sgn}(\tilde{h}) \tag{68}$$

$$\dot{\hat{q}} = \hat{M}_{yy} / I_0 - \alpha_2 \tilde{q} - k_q \,\mathrm{sgn}(\tilde{q}) \tag{69}$$

$$\dot{\hat{\gamma}} = \frac{\hat{L} + T\sin\hat{\alpha}}{mV} - \frac{(\mu - V^2 r)\cos\hat{\gamma}}{Vr^2} - \alpha_3 \tilde{h} - k_\gamma \,\mathrm{sgn}(\tilde{h}) \tag{70}$$

$$\dot{\hat{\alpha}} = \hat{q} - \dot{\hat{\gamma}} - \alpha_4 \tilde{q} - k_\alpha \,\mathrm{sgn}(\tilde{q}) \tag{71}$$

where,

$\hat{L} = \frac{1}{2}\rho V^2 S_0 \times 0.6203\hat{\alpha}$

$\hat{M}_{yy} = \frac{1}{2}\rho V^2 S_0 \bar{c}_0 [(-0.035\hat{\alpha}^2 + 0.036617\hat{\alpha} + 5.3261\times 10^{-6})$

$\quad + (\bar{c}_0 / 2V) q(-6.796\hat{\alpha}^2 + 0.3015\hat{\alpha} - 0.2289) + 0.0292(\delta_e - \hat{\alpha})]$

$\tilde{h} = \hat{h} - h$

$\tilde{q} = \hat{q} - q$

α_1, α_2, α_3 and α_4 are design constants, and k_h, k_q, k_γ and k_α are the sliding gains chosen by the designer.

The sliding surfaces of the observer are defined by $\boldsymbol{s}_o = [\tilde{h} \quad \tilde{q}]^T$. The average error dynamics during sliding where $\boldsymbol{s}_o = 0$ and $\dot{\boldsymbol{s}}_o = 0$ are:

$$\tilde{h} = 0 \tag{72}$$

$$\tilde{q} = 0 \tag{73}$$

$$V(\sin\hat{\gamma} - \sin\gamma) - k_h \,\mathrm{sgn}(\tilde{h}) = 0 \tag{74}$$

$$\begin{aligned}&(1/2I_0)\rho V^2 S_0 \bar{c}_0 \{-0.035(\hat{\alpha}^2 - \alpha^2) + [0.00742 - 0.3015(\bar{c}_0 / 2V)q]\tilde{\alpha} \\ &- 6.796(\bar{c}_0 / 2V) q(\hat{\alpha}^2 - \alpha^2)\} - k_q \,\mathrm{sgn}(\tilde{q}) = 0\end{aligned} \tag{75}$$

$$\dot{\tilde{\gamma}} = \frac{0.3102\rho V^2 S_0 \tilde{\alpha} + T(\sin\hat{\alpha} - \sin\alpha)}{mV} - \frac{(\mu - V^2 r)(\cos\hat{\gamma} - \cos\gamma)}{Vr^2} - k_\gamma \,\mathrm{sgn}(\tilde{h}) \tag{76}$$

$$\dot{\tilde{\alpha}} = -\dot{\tilde{\gamma}} - k_\alpha \,\mathrm{sgn}(\tilde{q}) \tag{77}$$

where,

$\tilde{\alpha} = \hat{\alpha} - \alpha$

$\tilde{\gamma} = \hat{\gamma} - \gamma$

The above error dynamics are nonlinear and difficult to analyze. Further simplification can be made however, by noting that in a hypersonic flight, the velocity V is high and the angle of attack α and flight path angle γ are typically very small justifying the following approximation:

$\sin\alpha \approx \alpha, \quad \sin\hat{\alpha} \approx \alpha$

$\cos\gamma, \quad \cos\hat{\gamma} \approx 1$

$\hat{\alpha}^2, \alpha^2 \approx 0$

$(\bar{c}_0 / 2V) q \approx 0$

An approximation for the local error dynamics can be derived from the nonlinear error dynamics of Eqs. (72-77) as:

$$\dot{\tilde{h}} = 0 \tag{78}$$

$$\dot{\tilde{q}} = 0 \tag{79}$$

$$\dot{\tilde{\gamma}} \approx -V(k_\gamma / k_h)\tilde{\gamma} + \{(0.3102\rho V^2 S_0 + T)/mV\}\tilde{\alpha} \tag{80}$$

$$\dot{\tilde{\alpha}} \approx \{-0.00371(k_\alpha / k_q)\rho V^2 S_0 \bar{c}_0 / I_0 - (0.3102\rho V^2 S_0 + T)/mV\}\tilde{\alpha} + V(k_\gamma / k_h)\tilde{\gamma} \tag{81}$$

When the trimmed conditions are substituted, the last two error equations can be further simplified as:

$$\dot{\tilde{\gamma}} \approx -15060(k_\gamma / k_h)\tilde{\gamma} + 0.0440\tilde{\alpha} \tag{82}$$

$$\dot{\tilde{\alpha}} \approx -\{0.8425(k_\alpha / k_q) + 0.044\}\tilde{\alpha} + 15060(k_\gamma / k_h)\tilde{\gamma} \tag{83}$$

The convergences of $\tilde{\gamma}$ and $\tilde{\alpha}$ depend on the ratios of k_γ / k_h and of k_α / k_q respectively. As a rule of thumb, the error dynamics of the observer on sliding surfaces $s_o = 0$ should be much faster than the tracking error dynamics, that is,

$$\min\{15060(k_\gamma / k_h),\ 0.8425(k_\alpha / k_q)\} >> \max\{\lambda_1, \lambda_2\}$$

In this study, $\lambda_1 = \lambda_2 = 0.4$, k_γ / k_h is chosen as 0.1 and k_α / k_q is chosen as 100, thus placing the poles of the reduced order error dynamics of Eqs. (82) and (83) at –1506 and –84.25. The simulation results in Figures 9 and 10 show the convergence behavior of the "off-line observer.", i.e., it is not being used for the sliding controller. Figure 9 shows that the errors converge to zero fast when no measurement noise is assumed. In Figure 10, the errors converge close to zero when a measurement noise with zero mean and standard deviation 100 ft and 0.15 deg/sec respectively is present. The results demonstrate that the sliding observer has good performance and exhibits robustness with respect to measurement noise.

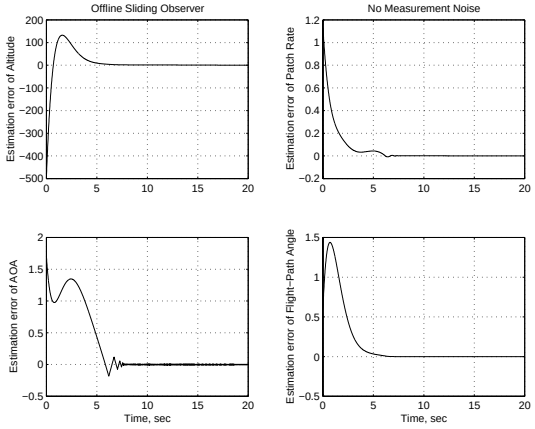

Figure 9 Offline Sliding Observer Without Measurement Noise

Initial State Errors: $\tilde{h}(0) = -500$ ft, $\tilde{q}(0) = 0.6$ deg/sec, $\tilde{\gamma}(0) = 0.6$ deg/sec, and $\tilde{\alpha}(0) = 1.72$ deg

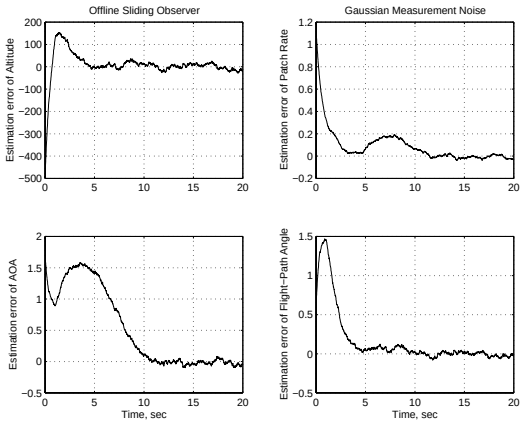

Figure 10 Offline Sliding Observer With Gaussian Measurement Noise
Initial State Errors: $\tilde{h}(0) = -500$ ft, $\tilde{q}(0) = 0.6$ deg/sec, $\tilde{\gamma}(0) = 0.6$ deg/sec, and $\tilde{\alpha}(0) = 1.72$ deg

ADAPTIVE SLIDING CONTROLLER-OBSERVER SYNTHESIS

In the previous sections we discussed the behavior of the adaptive sliding controller and of the sliding observer separately. In this section we combine the adaptive sliding controller with the observer to synthesize an adaptive sliding controller that does not require full state measurement as follows:

$$\hat{\boldsymbol{u}} = \begin{bmatrix} -v_1(\hat{\alpha},\hat{\gamma}) - k_1 \,\mathrm{sat}(s_1/\Phi_1) \\ -v_2(\hat{\alpha},\hat{\gamma}) - k_2 \,\mathrm{sat}(s_2/\Phi_2) \end{bmatrix} \tag{84}$$

$$\begin{bmatrix} \beta_c \\ \delta_e \end{bmatrix} = \begin{bmatrix} \hat{a} & 0 \\ 0 & \hat{b} \end{bmatrix} \begin{bmatrix} Y_{11} & Y_{12} \\ Y_{21} & Y_{22} \end{bmatrix}^{-1} \hat{\boldsymbol{u}} \tag{85}$$

$$\dot{\hat{a}} = -\frac{k_a}{\Delta} \boldsymbol{s}_\Delta^T \begin{bmatrix} Y_{11}Y_{22} & -Y_{11}Y_{12} \\ Y_{21}Y_{22} & -Y_{21}Y_{12} \end{bmatrix} \hat{\boldsymbol{u}} \tag{86}$$

$$\dot{\hat{b}} = -\frac{k_b}{\Delta} \boldsymbol{s}_\Delta^T \begin{bmatrix} -Y_{12}Y_{21} & Y_{11}Y_{12} \\ -Y_{22}Y_{21} & Y_{11}Y_{22} \end{bmatrix} \hat{\boldsymbol{u}} \tag{87}$$

$$\dot{\hat{h}} = V \sin\hat{\gamma} - \alpha_1 \tilde{h} - k_h \,\mathrm{sgn}(\tilde{h}) \tag{88}$$

$$\dot{\hat{q}} = \hat{M}_{yy}/I_0 - \alpha_2 \tilde{q} - k_q \,\mathrm{sgn}(\tilde{q}) \tag{89}$$

$$\dot{\hat{\gamma}} = \frac{\hat{L} + T\sin\hat{\alpha}}{mV} - \frac{(\mu - V^2 r)\cos\hat{\gamma}}{Vr^2} - \alpha_3 \tilde{h} - k_\gamma \,\mathrm{sgn}(\tilde{h}) \tag{90}$$

$$\dot{\hat{\alpha}} = \hat{q} - \dot{\hat{\gamma}} - \alpha_4 \tilde{q} - k_\alpha \,\mathrm{sgn}(\tilde{q}) \tag{91}$$

where, $v_1(\hat{\alpha},\hat{\gamma})$ and $v_2(\hat{\alpha},\hat{\gamma})$ are $v_1(\boldsymbol{x})$ and $v_2(\boldsymbol{x})$ in which α, γ substituted by $\hat{\alpha}$ and $\hat{\gamma}$.

The above controller is simulated for the same maneuvers and conditions as with previous controller. The simulation results are shown in Figures 11 and 12. It is seen that the adaptive sliding controller-observer provides good tracking despite parametric uncertainty.

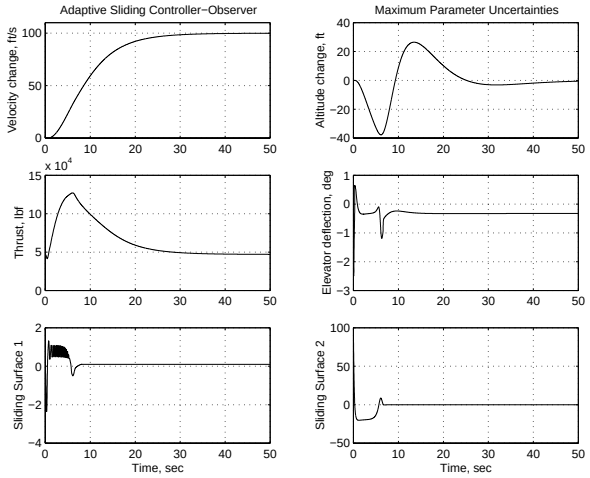

Figure 11 Adaptive Sliding Mode Controller-Observer
Response To A 100 ft/s Step Velocity Command With Maximum Parameter Uncertainties
Initial State Errors: $\tilde{h}(0) = -10$ ft, $\tilde{q}(0) = 0.15$ deg/sec, $\tilde{\gamma}(0) = 0.15$ deg/sec, and $\tilde{\alpha}(0) = 0.6$ deg

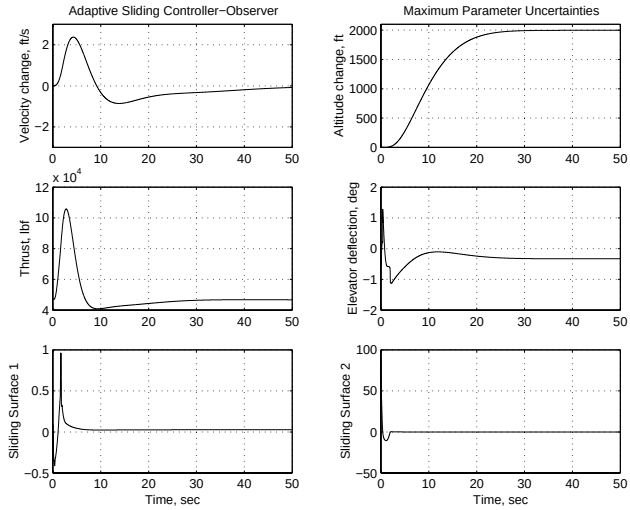

Figure 12 Adaptive Sliding Mode Controller-Observer
Response To A 2000 ft Step Altitude Command With Maximum Parameter Uncertainties
Initial State Errors: $\tilde{h}(0) = -10$ ft, $\tilde{q}(0) = 0.15$ deg/sec, $\tilde{\gamma}(0) = 0.15$ deg/sec, and $\tilde{\alpha}(0) = 0.6$ deg

CONCLUSION

In this paper, a MIMO adaptive sliding mode controller is designed for a nonlinear longitudinal model of a generic hypersonic vehicle. The controller is developed in several stages. First a sliding mode controller is developed using full sate feedback. Then the sliding mode controller is made adaptive in order to more efficiently deal with parametric uncertainty. A nonlinear sliding mode observer is developed to estimate the states that are not available for measurement. The combination of the observer with adaptive sliding mode controller led to the final adaptive sliding mode control design that uses only the states variables that are available for measurement in a typical hypersonic flight conditions. Simulations

demonstrate the efficiencies and robustness of the proposed controller for the longitudinal nonlinear model of the hypersonic vehicle in the presence of parametric uncertainty.

Acknowledgement

This work was supported by Air Force under grant #F49620-01-1-0489.

REFERENCES

[1] C. I. Marrison and R. F. Stengel*, Design of Robust control system for a hypersonic aircraft*, Journal of Guidance, Control, and Dynamics, Vol. 21, No. 1, 1998.

[2] Q. Wang and R. F. Stengel, *Robust Nonlinear Control of a Hypersonic Aircraft*, J. of Guidance, Control and Dynamics, Vol. 23, No. 4, 2000.

[3] J.-J. E. Slotine and W. Li, *Applied nonlinear control*, Prentice Hall, 1991

[4] B. Fernandez R. and J. K. Hedrick, *Control of Multivariable Non-linear Systems by the Sliding mode Method*, Int. J. Control, Vol. 46, No.3, 1987.

[5] J.-J. E. Slotine and J. A. Coetsee, *Adaptive Controller Synthesis for Nonlinear Systems*, Int. J. Control, Vol. 43, No. 6, 1986, pp. 1631-1651.

[6] J.-J. E. Slotine, J. K. Hedrick, and E. A. Misawa, *On Sliding Observers for Nonlinear Systems*, ASME Journal of Dynamics Systems, Measurement and Control, September 1987.

[7] J.K. Hedrick and W. H. Yao, *Adaptive Sliding Control of A Magnetic Suspension System*, Variable Structure Control For Robotics and Aerospace Applications, Edited by K.-K. D. Young, Elsevier Science Publishers B.V., 1993, pp 141-155.

[8] S. H. Zak, B. L. Walcott, and S. Hui, *Variable Structure Control and Observation of Nonlinear/Uncertain Systems*, Variable Structure Control For Robotics and Aerospace Applications, Edited by K.-K. D. Young, Elsevier Science Publishers B.V., 1993, pp. 59-88.

[9] P. A. Ioannou and J. Sun, *Robust Adaptive Control*, Prentice Hall, Upper Saddle River, 1996.